

Fractional-Order Memory-Reset Hybrid Integrator-Gain System - Part II Stability Analysis

Weise, C.; Wulff, K.; Hosseini, S. A.; Kaczmarek, M. B.; Hassan HosseinNia, S.; Reger, J.

10.1016/j.ifacol.2025.10.117

Publication date

Document Version Final published version

Published in IFAC-PapersOnline

Citation (APA)

Weise, C., Wulff, K., Hosseini, S. A., Kaczmarek, M. B., Hassan HosseinNia, S., & Reger, J. (2025). Fractional-Order Memory-Reset Hybrid Integrator-Gain System - Part II: Stability Analysis. *IFAC*-PapersOnline, 59(16), 283-288. https://doi.org/10.1016/j.ifacol.2025.10.117

Important note

To cite this publication, please use the final published version (if applicable). Please check the document version above.

Other than for strictly personal use, it is not permitted to download, forward or distribute the text or part of it, without the consent of the author(s) and/or copyright holder(s), unless the work is under an open content license such as Creative Commons.

Takedown policy

Please contact us and provide details if you believe this document breaches copyrights. We will remove access to the work immediately and investigate your claim.



ScienceDirect



IFAC PapersOnLine 59-16 (2025) 283-288

Fractional-Order Memory-Reset Hybrid Integrator-Gain System – Part II: Stability Analysis

C. Weise * K. Wulff * S. A. Hossein
i * M. B. Kaczmarek * * S. H. Hossein Nia * J. Reger *,1

* Control Engineering Group, Technische Universität Ilmenau, P.O. Box 10 05 65, D-98684, Ilmenau, Germany ** Department of Precision and Microsystems Engineering, Delft University of Technology, Delft, The Netherlands

Abstract: We consider the fractional-order version of the hybrid integrator-gain system (HIGS) including memory reset. For the implementation an explicit higher-order approximation is considered, which combines first-order reset elements with an integer-order HIGS. This framework can also be used for fractional-order extensions without memory reset. Using passivity theory we present a Circle-Criterion-like condition for the closed-loop stability based on this higher-order approximation.

Copyright © 2025 The Authors. This is an open access article under the CC BY-NC-ND license (https://creativecommons.org/licenses/by-nc-nd/4.0/)

1. INTRODUCTION

The hybrid integrator-gain system (HIGS) is a nonlinear switching control element which can overcome the limitations of linear control. For this reason it has been successfully applied to precision motion control (Deenen et al., 2017; Heertjes et al., 2017; Van Den Eijnden et al., 2024; Heertjes et al., 2023). The key feature of this loop-shaping element is a quasi linear describing function, which shows the amplitude response of a first-order low pass filter but the phase only drops to -38° , which allows for larger phase margins. As the element is passive the Circle Criterion can be applied to assess stability conservatively (Deenen et al., 2021).

In this paper we consider the fractional-order (FO) generalization of the HIGS introduced by Weise et al. (2025) including a memory reset. As in Hosseini et al. (2022) the order of integration provides an additional tuning parameter for loop shaping with the benefit of a lower reduced phase drop in the describing function for high frequencies. The memory reset simplifies the element as no additional 0-mode is required.

The main contribution of this work is the passivity analysis of the memory reset FO-HIGS by means of higher order approximations, which are inevitable for the online implementation of FO operators. We show that the same quadratic storage function can be used in both operation modes as a part of the approximation states is set to zero in the gain mode. This cannot be shown for the element presented in Hosseini et al. (2022) as the memory states do not vanish in the gain mode. Via passivity we derive a stability theorem based on the Circle Criterion which can be evaluated using measured frequency responses.

The remainder of this contribution is structured as follows. In Section 2 the required definitions of the applied FO operators are given. The following section introduces the

integer-order (IO) HIGS element as well as the FO version including the memory reset. In comparison to Hosseini et al. (2022) the memory of the FO operator is reset when re-entering the integration mode. In order to enable a strict implementation of both FO elements, higher-order approximations as a spacial discretization of the infinite state representation (Trigeassou et al., 2012) are introduced in Section 2.3. These approximations enable us to show the passivity of the new element using standard methods. The closed-loop stability can be shown via a Circle-Criterion-like theorem. Section 4 gives a simulation example before conclusions are drawn in Section 5.

2. PRELIMINARY RESULTS AND DEFINITIONS

In this section we recall the definition and basic poperties of the IO-HIGS element as well as its FO counterpart applying Caputo's definition.

2.1 Fractional-Order Operators

Non-integer order derivatives combine classical IO derivatives with the FO integral. We consider two approaches, following Podlubny (1999) for the integral of $f(\cdot)$ we have

$$t_0 \mathcal{I}^{\alpha} f(t) = \frac{1}{\Gamma(\alpha)} \int_{t_0}^t (t - \tau)^{\alpha - 1} f(\tau) d\tau, \quad t > t_0, \quad (1)$$

with the order of integration $\alpha \in \mathbb{R}^+$ and Euler's Gamma function $\Gamma(\cdot)$. For convenience we shall consider causal functions $f(\cdot) \in L^1_{loc}(\mathbb{R})$ with f(t) = 0 for all $t < t_0$, see (Matignon, 1996). A second approach is the infinite state (diffusive state) representation (Trigeassou et al., 2012; Trigeassou, 2019; Trigeassou and Maamri, 2019) given by

$$\dot{\zeta}(\omega, t) = -\omega \zeta(\omega, t) + f(t), \quad \omega \in [0, \infty)$$
 (2a)

$$\mathcal{I}^{\alpha} f(t) = \int_{0}^{\infty} \mu_{\alpha}(\omega) \zeta(\omega, t) d\omega, \quad \mu_{\alpha}(\omega) = \frac{\sin(\alpha \pi)}{\pi \omega^{\alpha}} \quad (2b)$$

with integral kernel $\mu_{\alpha}(\cdot)$ defined for $\alpha \in (0,1)$. The complete history of the function $f(\cdot)$ for $t < t_0$ can be

¹ Corresponding author: johann.reger@tu-ilmenau.de

lumped into the initial distribution of the state $\zeta(\omega, t_0)$. Applying the FO integral to an IO derivative of $f(\cdot)$ leads to Caputo's operator (Podlubny, 1999; Monje et al., 2010)

$$_{t_0} \mathcal{D}_t^{\alpha} f(t) = \frac{1}{\Gamma(m-\alpha)} \int_{t_0}^t \frac{f^{(m)}(t)}{(t-\tau)^{\alpha-m+1}} d\tau, \qquad (3)$$

where $\alpha \in \mathbb{R}^+$ is the differentiation order and m is an integer such that $m-1 \leq \alpha < m$. Due to the FO integral contained in this operator, the FO derivative has a memory and acts with respect to the time limits t_0 and t.

2.2 Integer- and Fractional-order HIGS

The IO-HIGS introduced by Deenen et al. (2017, 2021); Heerties et al. (2017) takes the form

$$\mathcal{H}_{\text{IO}}: \begin{cases} \dot{x}(t) = \omega_h e(t), & (e, \dot{e}, u) \in \mathcal{F}_{\text{IO}, 1} & (\text{I-Mode}) & (4a) \\ x(t) = k_h e(t), & (e, \dot{e}, u) \in \mathcal{F}_{\text{IO}, 2} & (\text{P-Mode}) & (4b) \\ u(t) = x(t) & (4c) \end{cases}$$

with $k_h > 0$ and $\omega_h > 0$ and the sector bounds defined by

$$\mathcal{F}_{\mathrm{IO},1} = \left\{ (e, \dot{e}, u) \in \mathbb{R}^3 | eu \ge \frac{1}{k_h} u^2 \wedge (e, \dot{e}, u) \notin \mathcal{F}_{\mathrm{IO},2} \right\}$$
$$\mathcal{F}_{\mathrm{IO},2} = \left\{ (e, \dot{e}, u) \in \mathbb{R}^3 | u = k_h e \wedge \omega_h e^2 > k_h e \dot{e} \right\}.$$

As long as the trajectories are located in the sector $\mathcal{F}_{\text{IO},1}$ the element acts as an integrator. Once the sector bound is hit $(u=k_h e)$ the element switches into the gain mode (P-Mode) and the state of the integrator follows the input e(t). The HIGS can be understood as a switching differential algebraic equation.

Generalizing this element towards FO integration is not straightforward, as the memory of the FO operators has to be considered. The memory-reset version given in Weise et al. (2025) reads

$$\tilde{\mathcal{H}}_{FO}: \begin{cases}
t_k \mathcal{D}_t^{\alpha} x(t) = \omega_h e(t), & (e, \dot{e}, u) \in \tilde{\mathcal{F}}_1 \\
x(t) = k_h e(t), & (e, \dot{e}, u) \in \tilde{\mathcal{F}}_2 \\
u(t) = x(t), & (5c)
\end{cases}$$
(5a)

where $t_k \mathcal{D}_t^{\alpha}$ denotes Caputo's derivative of order $\alpha \in (0, 1)$, $k_h > 0$, $\omega_h > 0$ and the memory reset instances t_k given by $(e(t_k^-), \dot{e}(t_k^-), u(t_k^-)) \in \tilde{\mathcal{F}}_2$, $(e(t_k^+), \dot{e}(t_k^+), u(t_k^+)) \in \tilde{\mathcal{F}}_1$

with the sector bounds illustrated in Fig. 1 (left) defined similar to the IO case above

$$\tilde{\mathcal{F}}_1 = \left\{ (e, \dot{e}, u) \in \mathbb{R}^3 \middle| eu \ge \frac{1}{k_h} u^2 \land (e, \dot{e}, u) \notin \tilde{\mathcal{F}}_2 \right\}
\tilde{\mathcal{F}}_2 = \left\{ (e, \dot{e}, u) \in \mathbb{R}^3 \middle| u = k_h e \land \omega_h e^2 > k_h e \left(\iota_k \mathcal{D}_t^{\alpha} e(t) \right) \right\}.$$

The second condition in $\tilde{\mathcal{F}}_2$ allows the re-entering of the integration mode if the trajectories are on the sector bound pointing inwards (see Fig.1). The resulting inequality in the input-output space can be reformulated with a time-derivative of arbitrary order

$$k_h < \frac{\partial u}{\partial e} = \frac{\dot{u}(t)}{\dot{e}(t)} = \frac{t_k \mathcal{D}_t^{\alpha} u(t)}{t_k \mathcal{D}_t^{\alpha} e(t)} = \frac{\omega_h e(t)}{t_k \mathcal{D}_t^{\alpha} e(t)}, \quad \text{for} \quad e > 0.$$

As long as the trajectories remain in the sector $\tilde{\mathcal{F}}_1$ the FO integration uses the time instant of entering the integration mode t_k as a lower limit in (5a). Thus memory is accumulated and it is only reset when the gain-mode $(\tilde{\mathcal{F}}_2)$ has been active in between.

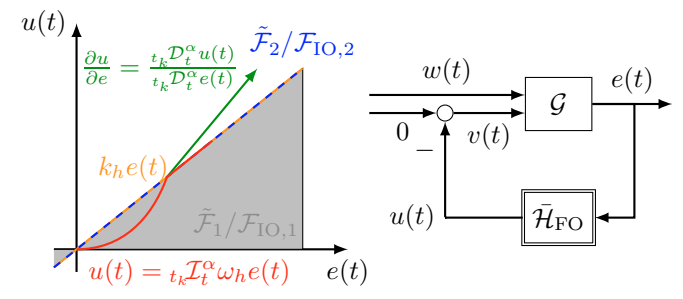


Fig. 1. Sector bounds of the FO-HIGS (IO-HIGS) in the input-output plane (left) and Lur'e system (right).

2.3 Diffusive State Truncation

As FO operators are non-local the implementation requires a truncation of its memory. Besides the application of the well-known short memory principle (see (Podlubny, 1999)) higher-order LTI systems can be used to approximate the desired behavior in a certain frequency range. A typical approximation can be derived by applying Oustaloup's formula to obtain a Padé approximation of the FO term in the Laplace domain (see (Monje et al., 2010)). We derive the approximation by lumping the distributed state space of (2a) into a finite dimensional LTI system.

Direct Approximation In order to approximate the FO integral we use a spacial discretization of the positive halfline $\omega \in [0, \infty)$ by selecting N frequencies $0 = \omega_1 < \omega_2 < \cdots < \omega_N < \infty$. Choosing $\omega_1 = 0$ includes the pure IO integration as the kernel $\mu_{\alpha}(\cdot)$ in (2b) is weakly singular at $\omega = 0$. Hence the FO integral is approximated by an LTI system of order N:

$$\dot{z}(t) = \bar{A}_z z(t) + \bar{B}_z \omega_h e(t)$$
 (6a)

$$\omega_h \mathcal{I}^{\alpha} e(t) \approx u(t) = \bar{C}_z z(t),$$
 (6b)

with $\bar{A}_z = -\operatorname{diag}(\omega_1 \cdots \omega_N), \ \bar{B}_z^{\top} = (1 \cdots 1) \text{ and } \bar{C}_z = (c_1 \ c_2 \cdots c_N), \ c_i > 0 \text{ for } i = 1, \dots, N.$

Remark 1. The coefficients c_i scaling the individual modes ω_i of the approximation can be derived from the kernel $\mu_{\alpha}(\omega)$ in (2b). Typically the individual modes ω_i are chosen equidistant in a logarithmic scale within a certain frequency band of interest. The coefficients c_i result from the integration of the kernel $\mu_{\alpha}(\omega)$

$$c_{i} = \int_{\underline{\omega}_{i}}^{\bar{\omega}_{i}} \mu_{\alpha}(\omega) d\omega = \frac{\sin(\alpha\pi)}{(1-\alpha)\pi} \left[\bar{\omega}_{i}^{1-\alpha} - \underline{\omega}_{i}^{1-\alpha} \right], \quad (7)$$

with $\underline{\omega}_i = \sqrt{\omega_i \omega_{i-1}}$, $\bar{\omega}_i = \sqrt{\omega_i \omega_{i+1}}$ for $i = 1, \ldots, N$ and $\omega_0 = 0$. As the integral of the kernel (2b) does not converge if the upper limit tends to infinity, the approximation is limited in the higher frequency range and the coefficient c_N scaling this mode can only take into account the frequencies up to $m\omega_N = \omega_{N+1}$ (m > 0).

In addition to that standard approximations of FO operators like the Oustaloup-filter or its refined version (Monje et al., 2010; Tepljakov et al., 2011) can be used to obtain the coefficients c_i , as all these approximations are based on real poles and therefore system (6) is a modal state-space representation of these transfer functions with a normalized input matrix.

With (6) and the slightly changed sectors $\bar{\mathcal{F}}_1$, $\bar{\mathcal{F}}_2$, the FO-HIGS element with memory reset is approximated by

$$\bar{\mathcal{H}}_{FO}: \begin{cases} \dot{z}(t) = \bar{A}_z z(t) + \bar{B}_z \omega_h e(t), & (e, \dot{e}, u) \in \bar{\mathcal{F}}_1 \quad (8a) \\ z(t) = \binom{k_h (c_1)^{-1}}{0_{N-1}} e(t), & (e, \dot{e}, u) \in \bar{\mathcal{F}}_2 \quad (8b) \\ u(t) = \bar{C}_z z(t), & (8c) \end{cases}$$

$$\begin{split} \bar{\mathcal{F}}_1 &= \left\{ (e, \dot{e}, u) \in \mathbb{R}^3 | eu \ge \frac{1}{k_h} u^2 \wedge (e, \dot{e}, u) \not\in \bar{\mathcal{F}}_2 \right\} \\ \bar{\mathcal{F}}_2 &= \left\{ (e, \dot{e}, u) \in \mathbb{R}^3 | u = k_h e \wedge b_N \omega_h e^2 > k_h e \dot{e} \right\}, \end{split}$$

and
$$b_N = \sum_{i=1}^N c_i,$$
 $c_i > 0, \quad k_h > 0.$ (9)

The memory is captured in the states z_2 to z_N and in the P-mode $(e, \dot{e}, u) \in \mathcal{F}_2$ it is reset to zero. The first state is given by the pure proportional term $z_1(t) = \frac{k_h}{c_0} e(t)$ such that the output is continuous at the switching instant. The solution $z(\cdot)$ exists for all $t > t_0$ for all initial conditions satisfying $\bar{C}_z z(t_0) \leq k_h e(t_0)$ and inputs $e(\cdot) \in L^2_{loc}(\mathbb{R})$. Note that the states are set to zero if the input vanishes, i.e. e = 0. This happens either in $\bar{\mathcal{F}}_2$ directly or in $\bar{\mathcal{F}}_1$ as \bar{C}_z has only positive elements and the system is zero-state observable, Khalil (1996). As a consequence the individual states z_i have always the same sign. Since the input matrix \bar{B}_z has only positive elements the input e determines the sign of each state, i.e. $sign(e) = sign(z_i)$ for all i = 1, ..., n. Remark 2. This state space representation is not suitable for the implementation of the FO-HIGS without memory reset. When the memory is not set to zero, the dynamics of the last N-1 states remain unchanged in the P-mode and these states are therefore nonzero. As a consequence the output matrix \bar{C}_z has to be switched into the second mode, i.e. $u(t) = (c_1 \ 0) z(t)$ with $(e, \dot{e}, u) \in \mathcal{F}_2$. As the switching condition $(e, \dot{e}, u) \in \mathcal{F}_2$ depends on the output u itself, this leads to an algebraic loop.

Indirect Approximation For a second approach to implement the FO integral of order α we split the FO integral, such that the integrating behavior is guaranteed for the low frequency range as demonstrated in Weise et al. (2025). For this split we apply Caputo's operator: $\mathcal{I}^{\alpha}f(t) = \mathcal{I}^{1}\left(\mathcal{D}^{1-\alpha}f(t)\right) = \mathcal{I}^{1}\left(\mathcal{I}^{\alpha}\left(\mathcal{D}^{1}f(t)\right)\right)$. Applying the distributed state representation (2) we obtain for $u(t) = x_I(t) = \mathcal{I}^{\alpha}(\omega_h e(t))$:

$$\dot{\zeta}(\omega, t) = -\omega \zeta(\omega, t) + \omega_h \dot{e}(t) \qquad (10a)$$

$$\dot{\zeta}(\omega, t) = -\omega \zeta(\omega, t) + \omega_h \dot{e}(t) \qquad (10a)$$

$$\dot{x}_I(t) = \mathcal{D}^{1-\alpha} (\omega_h e(t)) = \int_0^\infty \mu_\alpha(\omega) \zeta(\omega, t) d\omega. \qquad (10b)$$

We can rewrite (10a) with the new distributed state $x_{\zeta}(\cdot)$: $\mathbb{R}^+ \times \mathbb{R}^+ \to \mathbb{R}$ and distributed output $\zeta(\cdot) : \mathbb{R}^+ \times \mathbb{R}^+ \to \mathbb{R}$ $(\omega \in [0,\infty))$ using a feedthrough term

$$\dot{x}_{\zeta}(\omega, t) = -\omega x_{\zeta}(\omega, t) + \omega_{h} e(t) \qquad (11a)$$

$$\zeta(\omega, t) = -\omega x_{\zeta}(\omega, t) + \omega_{h} e(t) \qquad (11b)$$

$$\zeta(\omega, t) = -\omega x_{\zeta}(\omega, t) + \omega_h e(t) \qquad (11b)$$

$$\dot{x}_I(t) = \mathcal{D}^{1-\alpha} \left(\omega_h e(t) \right) = \int_0^\infty \mu_\alpha(\omega) z(\omega, t) d\omega. \tag{11c}$$

Remark 3. Equations (11) show that Caputo's operator can be implemented causally for $\alpha \in (0, 1)$.

To approximate the distributed dynamics in x_{ζ} , we use the same frequencies as above: $0 < \omega_2, \ldots, \omega_N < \infty$. As the integrator ($\omega_1 = 0$) is separated, the mode $\omega_1 = 0$ is not included to approximate the output (11c). This results in

$$\dot{z}_M(t) = A_z z_M(t) + B_z \omega_h e(t) \tag{12a}$$

$$\dot{z}_I(t) = C_z A_z z_M(t) + b_N \omega_h e(t) \qquad (12b)$$

$$\omega_h \mathcal{I}^\alpha e(t) \approx u(t) = z_I(t)$$
 (12c)

with $A_z = -\operatorname{diag}(\omega_2 \cdots \omega_N)$, $B_z = (1 \cdots 1)^{\top}$ and positive coefficients $c_i > 0, i = 2, \dots, N$ given by (7) and b_N given by (9). In this approximation the state $z_M \in \mathbb{R}^{N-1}$ represents the memory of the FO operator and the single IO integration guarantees a continuous output. This new state can also be interpreted as a transformed version of the direct approximation

$$\begin{pmatrix} z_M \\ z_I \end{pmatrix} = \begin{pmatrix} 0 & I \\ c_0 & C_z \end{pmatrix} z = Tz.$$
 (13)

Now we are able to approximate both FO hybrid elements in terms of the LTI system (12) without algebraic constraints.

The FO-HIGS with memory reset can be approximated with the following LTI approximation similar to the approximation presented by Weise et al. (2025):

$$\tilde{\mathcal{H}}_{\mathrm{FO'}} \begin{cases} \left(\dot{z}_{M}(t)\right) = \left(A_{z}z_{M}(t) + B_{z}\omega_{h}e(t)\right), & (e,\dot{e},u) \in \bar{\mathcal{F}}_{1} \\ C_{z}z_{M}(t) + D_{z}\omega_{h}e(t) \end{pmatrix}, & (I\text{-mode}) \\ \left(z_{M}(t)\right) = \left(\begin{matrix} 0 \\ k_{h}e(t) \end{matrix}\right), & (e,\dot{e},u) \in \bar{\mathcal{F}}_{2} \\ (P\text{-mode}) \end{cases}$$

$$u(t) = z_{I}(t).$$

In this implementation the memory states z_M are set to zero as the element is in the gain-mode $((e, \dot{e}, u) \in \bar{\mathcal{F}}_2)$. Therefore this IO approximation combines N-1 first-order reset elements with an integrator. As the reset condition is given in terms of the in- and output of the element, however, it does not show the same behavior as a series connection of first-order reset elements and an IO-HIGS.

3. STABILITY ANALYSIS

In this part we generalize the stability results presented in Deenen et al. (2017) for the IO-HIGS towards the approximation of the FO-HIGS element $\bar{\mathcal{H}}_{FO}$. The sectorboundedness of the input-output behavior allows for a stability analysis in the frequency domain.

3.1 Passivity Analysis

Although the reset of the state leads to partial hybrid dynamics, we are able to use classic passivity definitions as applied in Carrasco et al. (2010) to reset control systems. Definition 4. (Passivity (van der Schaft, 2017)). Let $\mathcal{L}_{2,e}$ denote the extended \mathcal{L}_2 -space. A system $\overline{\mathcal{H}}: \mathcal{L}_{2,e} \to \mathcal{L}_{2,e}$

$$\bar{\mathcal{H}}: \left\{ \begin{array}{ll} \dot{x} = f(x, u), & u \in \mathbb{R} \\ y = h(x, u), & y \in \mathbb{R} \end{array} \right. \tag{15a}$$

is passive if there exists a positive semidefinite storage function V = V(x), such that for all initial conditions and any input $u(\cdot)$ the following inequality holds for all $t \geq t_0$

$$V(x(t)) - V(x(t_0)) \le \int_{t_0}^t S(u(\tau), y(\tau)) d\tau,$$
 (16)

where the supply rate is defined as S(u, y) = uy.

In comparison to the passivity definition given in Khalil (1996) we require the integral version of the dissipation inequality, as the states z of the memory reset FO-HIGS jump when it changes from I- to P-mode.

Lemma 1. The approximation of the FO-HIGS element $\bar{\mathcal{H}}_{FO}$ with $\omega_h, k_h > 0$, modes $\omega_i > 0$ for i = 2, ..., N, and positive constants $c_i > 0$ for i = 1, ..., N is passive.

Proof. To prove the passivity of the approximation $\overline{\mathcal{H}}_{FO}$ we use the modal coordinates given in (6). Consider the storage function $V(z) = \frac{\kappa_1}{2}u^2 + \frac{\kappa_2}{2}\sum_{i=2}^N c_i z_i^2$, i.e.

$$V(z) = \frac{\kappa_1}{2} z^{\top} \left(\bar{C}_z^{\top} \bar{C}_z \right) z + \frac{\kappa_2}{2} z^{\top} M z = z^{\top} \bar{P} z > 0. \quad (17)$$
with $\kappa_1, \kappa_2 > 0$ and $M = \text{diag}(0, \text{diag}(C_z)).$

If $\bar{\mathcal{H}}_{FO}$ is strictly passive in each mode and the storage function V decreases at the instances of state-reset, then $\bar{\mathcal{H}}_{FO}$ is passive, see Carrasco et al. (2010).

The derivative of the storage function in the I-mode is

$$\begin{split} \dot{V}(z)|_{\mathrm{I}} &= \kappa_1 u \, \bar{C}_z \dot{z} + \kappa_2 \sum_{i=2}^N c_i z_i (-\omega_i z_i + \omega_h e) \\ &= z^{\mathsf{T}} \Big(\kappa_1 \bar{C}_z^{\mathsf{T}} \bar{C}_z \bar{A}_z + \kappa_2 \operatorname{diag}(\bar{C}_z) \bar{A}_z \Big) z + \kappa_2 \omega_h e \sum_{i=2}^N c_i z_i \\ &= -z^{\mathsf{T}} \bar{Q}z + \kappa_2 \omega_h e u - \kappa_2 \omega_h e c_1 z_1, \end{split}$$

where $\bar{Q} = -\kappa_1 \bar{C}_z^{\top} \bar{C}_z \bar{A}_z - \kappa_2 \operatorname{diag}(\bar{C}_z) \bar{A}_z$. While \bar{Q} is indefinite, we still have $z^{\top} \bar{Q} z \geq 0$ as all components z_i have the same sign $i = 1, \ldots, n$. Note that $\omega_1 = 0$ in \bar{A}_z , thus is independent of the first state z_1 . The second term in \dot{V} represents the required supply rate S(e, u) = eu. Recall that the states z_1 have the same sign as the error e. Thus the last term is also negative.

To show the strict passivity (following the definition given in Khalil (1996)) in the integration mode we apply the sector condition given by $\bar{\mathcal{F}}_1$. For e>0 we use $k_he\geq u=Cz$ leading to $e\geq k_h^{-1}Cz$ and

$$\dot{V}(z)|_{\mathrm{I}} \le -z^{\mathsf{T}} \bar{Q}z - \frac{\kappa_2 \omega_h}{k_h} Cz \, c_1 z_1 + \kappa_2 \omega_h eu. \tag{18}$$

For e < 0 we have $e \le k_h^{-1}Cz$ and obtain the same result. With the choice $\kappa_2 = \omega_h^{-1}$ the integration mode is strictly passive (Khalil, 1996), i.e.

$$\dot{V}(z)|_{\mathbf{I}} \leq -z^{\top} \bar{Q}z - \phi_2(z) + eu$$
 with $\phi_2(z) = \frac{1}{k_h} z^{\top} C^{\top} (c_1 \ 0) z$, where $z^{\top} \bar{Q}z + \phi_2(z) \geq 0$.

In the P-mode the same storage function (17) is applied. As the states z_i for $i=2,\ldots,N$ are zero the storage function (17) simplifies to $V(z)|_{\rm P}=\frac{\kappa_1}{2}u^2=\frac{\kappa_1}{2}c_1^2z_1^2$ and

$$\dot{V}(z)|_{P} = \kappa_1 c_1^2 z_1 \dot{z}_1 = \kappa_1 c_1 k_h u \dot{e},$$

as $z_1=\frac{k_h}{c_1}e$. From the region condition in $\bar{\mathcal{F}}_2$ we obtain $b_N\omega_heu>k_h\dot{e}u$. Adding zero yields

$$\dot{V}(z)|_{\mathbf{P}} \leq \kappa_1 c_1 b_N \omega_h e u + \frac{\kappa_3}{k_h} u^2 - \frac{\kappa_3}{k_h} c_1^2 z_1^2 - z^\top \bar{Q} z
\leq (\kappa_1 c_1 b_N \omega_h + \kappa_3) e u - \left(\frac{\kappa_3}{k_h} C z c_1 z_1 + z^\top \bar{Q} z\right).$$

Choosing $\kappa_1, \kappa_3 > 0$ such that $(\kappa_1 c_1 b_N \omega_h + \kappa_3) = 1$ yields a similar form as in the integration mode

$$\dot{V}(z)|_{\mathcal{P}} \le eu - z^{\top} \bar{Q}z - \kappa_3 \phi_2(z). \tag{19}$$

Therefore the approximation of the FO-HIGS is also strictly passive in the gain mode. With $\kappa_3 < 1$ the right-hand side in (19) is also an upper bound on the derivative in the I-mode.

The state z is discontinuous when changing from the integration to the gain mode. The value of the storage function decreases at these switching instances since

$$V(z(t_k^+)) - V(z(t_k^-)) = \frac{\kappa_1}{2} u^2 - \left(\frac{\kappa_1}{2} u^2 + \frac{\kappa_2}{2} z^\top M z\right) = -\frac{\kappa_2}{2} z^\top M z \le 0.$$
 (20)

Hence the dissipation inequality (16) is satisfied in both modes. This concludes the proof.

The proof does not require the constants c_i to approximate the original FO operator, hence the parameters c_i might also be used to tune any hybrid element.

Note that the storage function (17) cannot be used to show the passivity of system $\hat{\mathcal{H}}_{FO}$ (without memory reset) as the memory states z_i with $i=2,\ldots,N$ do not vanish in the P-mode.

3.2 Circle-Criterion-like Condition

Consider closed-loop Lur'e type interconnection in Fig. 1 (right) with the passive linear plant

$$\dot{x}_p(t) = A_p x_p(t) + B_{pv} v(t) + B_{pw} w(t)$$
 (21a)

$$e(t) = C_p x_p(t) \tag{21b}$$

$$(G(s) \ G_{ew}(s)) = C_p (sI - A_p)^{-1} (B_{pv} \ B_{pw}). \tag{21c}$$

Definition 5. (ISS (Khalil, 1996)). The system (15a) is called input-to state stable (ISS), if there exist a class \mathcal{KL} -function $\beta(\cdot,\cdot)$ and a class \mathcal{K} -function $\gamma(\cdot)$, such that for any initial condition $x(t_0)$ and any bounded input u, the solution x exists and satisfies for all $t \geq t_0$

$$||x(t)|| \le \beta(||x(t_0)||, t - t_0) + \gamma \sup_{t_0 \le \tau \le t} ||u(\tau)||.$$

Theorem 6. Consider the system (21) in feedback with the approximation of the FO-HIGS with memory reset $\bar{\mathcal{H}}_{FO}$ in (8) with $k_h > 0$ and $\omega_h > 0$ as depicted in Fig. 1. This feedback system is ISS with respect to the input w, if A_p is Hurwitz and the transfer function G(s) satisfies

$$\operatorname{Re}\left\{G(\mathrm{j}\omega)\right\} > -\frac{1}{k_h} \quad \text{for all} \quad \omega \in \mathbb{R} \cup \{\pm \infty\}.$$
 (22)

Proof. The proof follows the ideas presented in Deenen et al. (2021). We apply the Kalman–Yakubovich-Popov (KYP) lemma (Khalil, 1996) in combination with the storage function (17) of Lemma 1 to generate a common (quadratic) ISS Lyapunov function.

As the stable process with the minimal realization given by (21) satisfies condition (22), the KYP lemma establishes the existence of L, $P = P^{\top} > 0$, and $\varepsilon_p > 0$ such that

$$A_p^\top P + P A_p^\top = -L^\top L - \varepsilon_p P, \quad P B_{pw} = C_p^\top - \sqrt{\frac{2}{k_h}} L^\top.$$

The corresponding Lyapunov function $V_p(x_p) = x_p^\top P x_p$ satisfies $\underline{\lambda}(P) \|x_p\|^2 \leq V_p(x_p) \leq \overline{\lambda}(P) \|x_p\|^2$ with the minimal and maximal eigenvalue $\underline{\lambda}(P)$ and $\overline{\lambda}(P)$ of the matrix P, respectively. For the derivative of V_p along the solution of the closed-loop system in Fig. 1 and following the steps in van Loon et al. (2017) yields

$$\dot{V}_p(x_p) \le -\left(\varepsilon_p \bar{\lambda}(P) - \frac{1}{\delta_1}\right) \|x_p\|^2 + \delta_1 \left(\bar{\lambda}(P) \|B_{gw}\|\right)^2 \|w\|^2.$$
 For sufficiently large $\delta_1 > 0$ we have $\kappa_6 := \varepsilon_p \bar{\lambda}(P) - \frac{1}{\delta_1} > 0$.

The upper bound of the derivative of the storage function (19) can be modified applying Young's inequality and $||u|| \le k_h ||e||$ leading to

$$\dot{V}(z) \le -\left\|\frac{\kappa_3}{k_h}C^{\top}(c_10) + \bar{Q}\right\|\|z\|^2 + \left(\frac{\delta_3}{2}k_h^2 + \frac{1}{2\delta_3}\right)\|e\|^2$$

for some $\delta_3 > 0$. With $\kappa_4 := \left\| \frac{\kappa_3}{k_h} C^{\top}(c_1 0) + \bar{Q} \right\| > 0$, $\kappa_5 := \frac{\delta_3}{2} k_h^2 + \frac{1}{2\delta_3} > 0$ and substituting (21b) yields

$$\dot{V}(z) \le -\kappa_4 \|z\|^2 + \kappa_5 \|C_n\| \|x_n\|^2. \tag{23}$$

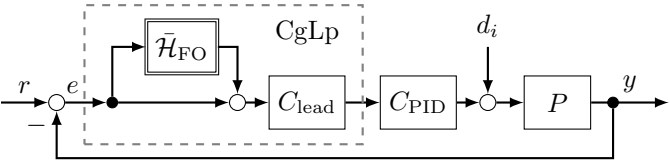


Fig. 2. Block diagram of the closed-loop system.

Now we combine both functions to construct the Lyapunov function of the closed loop with $x_{cl} = \begin{pmatrix} x_p^\top & z^\top \end{pmatrix}^\top$, i.e.

$$V_{\rm cl}(x_p,z) = V_p(x_p) + \mu V(z) = x_{\rm cl}^\top \begin{pmatrix} P & 0 \\ 0 & \mu \bar{P} \end{pmatrix} x_{\rm cl} \geq 0$$

with $0 < \mu < \kappa_6(\kappa_5 ||C_p||)^{-1}$ which is positive definite and radially unbounded. Finally the upper bound on the time derivative satisfies

$$\dot{V}_{\text{cl}}(x_p, z) \leq -\delta_4 \|x_{\text{cl}}\|^2 + \delta_1 \left(\bar{\lambda}(P) \|B_{gw}\|\right)^2 \|w\|^2$$
 with $\delta_4 = \min\left(\kappa_6 - \mu \kappa_5 \|C_p\|, \mu \kappa_4\right)$, almost everywhere.

As the Lyapunov function only combines the storage function (17) with a quadratic term of the process states we have according to (20)

$$V_{\rm cl}(x_{\rm cl}(t_k^+)) - V_{\rm cl}(x_{\rm cl}(t_k^-)) = -\frac{\kappa_2}{2} z^{\mathsf{T}} Mz \leq 0,$$
 hence input-to-state stability according to Definition 5. \square

This approach is rather conservative regarding the stability results, as it mostly exploits the passivity of the process and the hybrid element. Therefore the gain parameter k_h has the main influence on the results. Future analysis should focus on approaches similar to the partitioning ideas presented by Deenen et al. (2021) and Van Den Eijnden et al. (2024) for the IO-HIGS.

4. SIMULATION EXAMPLE

Our example demonstrates the potential performance enhancement of FO-HIGS in a control system and the analysis of the closed-loop stability using the proposed method.

The plant P consists of a second-order transfer function and a pole-zero pair approximating a delay $T_d = 0.0015 \,\mathrm{s}$

$$P(s) = \frac{\omega_n^2}{s^2 + 2\zeta\omega_n s + \omega_n^2} \frac{-T_d s + 1}{T_d s + 1}, \quad \omega_n = 5, \\ \zeta = 0.2.$$
 (24)

We consider tracking control of the reference $r(t) = \sin(15t)$ subject to the input disturbance $d_i(t) = 0.1 \sin(40t)$. Since the plant exhibits a large phase-drop at high frequencies, the bandwidth is limited. The following PID controller achieves a phase margin $\phi_r = 30^{\circ}$ at $\omega_c = 100 \,\text{rad/s}$:

$$C_{\text{PID}}(s) = k_p \left(1 + \frac{\omega_i}{s} \right) \left(\frac{s/\omega_d + 1}{s/\omega_t + 1} \right), \tag{25}$$

where $k_p=115.5$, $\omega_i=\omega_c/5$ is the frequency at which integral action stops, differentiating action starts at $\omega_d=\omega_c/a$ and terminates at $\omega_t=a\omega_c$, where we choose a=3.4 to achieve the phase margin. Note that the integral frequency ω_i , and thus tracking and disturbance rejection, is limited to $20\,\mathrm{rad/s}$ due to the phase lag.

To compensate some phase lag that allows to increase the integral frequency ω_i we add a so-called Constant-in-gain Lead-in-phase (CgLp) element, see Fig. 2. For comparison we devise two CgLp elements using an IO-HIGS and FO-HIGS element, respectively. For C_{lead} we choose the inverse of the base linear transfer function of $(1 + \bar{\mathcal{H}}_{\text{FO}})$ given by

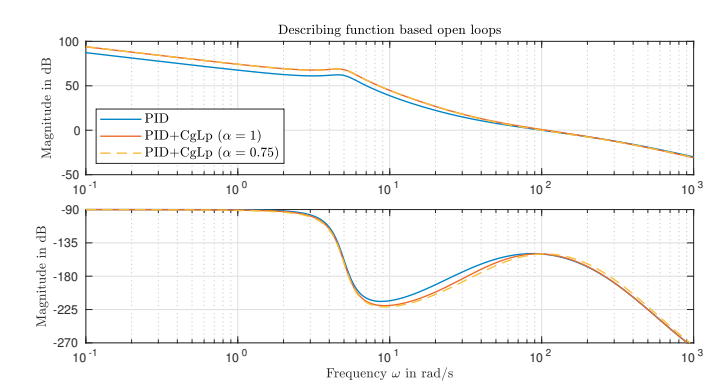


Fig. 3. Open loop frequency responses.

$$C_{\text{lead}}(s) = \frac{(1+s/w_{rh})^{\alpha}}{(1+s/w_{rh})^{\alpha}+k_{h}}.$$
 (26)

For $\alpha=1$, $C_{\rm lead}(s)$ acts as an integer lead, compensating the gain of the IO-HIGS; for $\alpha\in(0,1)$ it can compensate the gain of the FO-HIGS element. In the latter case we use a third-order transfer function to approximate the FO $C_{\rm lead}(s)$ for the stability analysis and implementation in the time-domain.

For tuning of this PID+CgLp controller we first elevate the integral frequency ω_i from 20 rad/s to 50 rad/s ensuring sufficient gain at low frequencies. This introduces a 15° phase lag at $\omega_c=100\,\mathrm{rad/s}$, which we aim to compensate with the CgLp element. For the IO-HIGS ($\alpha=1$) we choose $k_h=2.2$ and $\omega_h=40$. For the FO-HIGS we choose $\alpha=0.75, k_h=2.2$, and $\omega_h=18$, to maintain a constant gain across all frequencies and achieve a phase lead of 15° at $\omega_c=100\,\mathrm{rad/s}$ for the describing function of the CgLp element. The frequency responses for the openloops with the three controllers (PID and PID+CgLp with IO-/FO-HIGS) are shown in Fig. 3. In order to achieve a comparable crossover frequency the controller gain with either CgLp element is adjusted to $\tilde{k}_p=99.17$.

As the nonlinear controllers are designed using their describing function, with higher-order harmonics neglected, we analyse the performance of the three control loops using the normalized cumulative power spectrum density (CPSD) shown in Fig. 4. Recognizing that higher-order harmonics can propagate through all frequency ranges, CPSD analysis can help to observe their effect on the error. In Fig. 4, the reduction in error related to reference tracking and disturbances is evident in the nonlinear controllers. This reduction is attributed to their gain advantage at low frequencies while maintaining the phase consistent at the bandwidth frequency. Additionally, minor jumps observed in the PID+CgLp cases can be attributed to higher-order harmonics. Nevertheless, these higher-order harmonics do not significantly impact the system performance. Despite the slightly better performance of the FO-HIGS controller in this example, we cannot conclusively establish the superiority of the introduced FO-HIGS filter in terms of performance based solely on this case. Here, we analyzed the two controllers side by side to demonstrate that this new filter not only performs comparably but also has the potential to outperform the existing IO-HIGS. However, the key advantage of the FO-HIGS lies in its tunability and its applicability in scenarios where the degree of nonlinearity introduced into the system is critical.

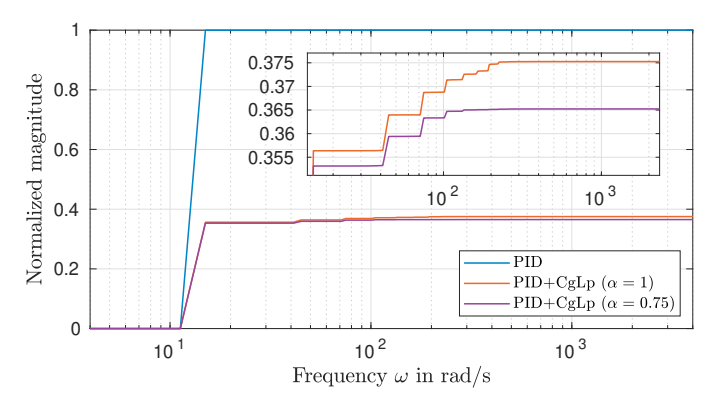


Fig. 4. Normalized cumulative power spectrum density of the closed-loop error.

To assess the stability of the FO-HIGS-based controller, we utilize Theorem 6. Fig. 5(a) shows the Nyquist plot of $L = C_{\text{lead}} C_{\text{PID}} P$ establishing that A_p is Hurwitz. In Fig. 5(b) the Nyquist plot of $G = \frac{L}{1+L}$ is shown. We observe that (23) is satisfied for $k_h < 3.37$. Furthermore, we have $\text{Re}\{G(\text{j}\infty)\} > -\frac{1}{k_h}$ for all $k_h > 0$ as G is strictly proper. Therefore, with Theorem 6, the closed-loop system of Fig. 2 is ISS for all $k_h < 3.37$ and $\omega_h \in (0, \infty)$.

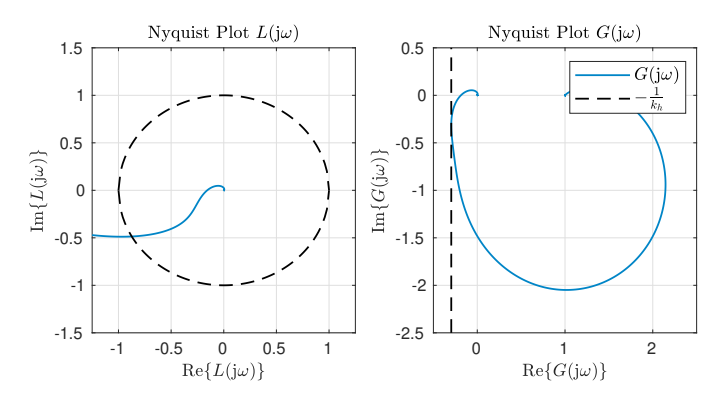


Fig. 5. Nyquist diagram of L (left) and G (right).

5. CONCLUSIONS

In this contribution we investigate the passivity of the FO-HIGS element with memory reset. The reset of the infinite memory simplifies the FO-HIGS element as only the gain and integration mode are present. As the possible negative memory is deleted, the trajectories cannot leave the sector at the lower limit $(u\!=\!0)$, hence the 0-mode is not required.

We derive a direct approximation based on the infinite state representation of the FO integral. The resulting higher order approximation contains the actual memory in the state z_M whereas the continuous output of the FO integration is given by the state z_I . When the output z_I crosses the sector bound, the states z_M are set to zero. So we may apply the same storage function in I- and P-mode to show strict passivity of the element. The approximations combine first-order reset elements with an IO-HIGS, thus, the results are not limited to the original FO integration. Based on passivity we provide a Circle-Criteria-like condition to guarantee ISS in closed loop.

REFERENCES

Carrasco, J., Baños, A., and Schaft, A. (2010). A passivity-based approach to reset control systems stability. Systems and Control Letters, 59, 18–24.

Deenen, D., Heertjes, M., Heemels, W., and Nijmeijer, H. (2017). Hybrid integrator design for enhanced tracking in motion control. In *American Control Conference*, 2863–2868.

Deenen, D.A., Sharif, B., van den Eijnden, S., Nijmeijer, H., Heemels, M., and Heertjes, M. (2021). Projection-based integrators for improved motion control: Formalization, well-posedness and stability of hybrid integrator-gain systems. *Automatica*, 133, 109830.

Heertjes, M., Eijnden, S.V.D., and Sharif, B. (2023). An Overview on Hybrid Integrator-Gain Systems with applications to Wafer Scanners. In *IEEE International Conference on Mechatronics*, 1–8.

Heertjes, M., Irigoyen, N., and Deenen, D. (2017). Datadriven tuning of a hybrid integrator-gain system. In *IFAC World Congress*, 10851–10856.

Hosseini, S.A., Tavazoei, M.S., Van Eijk, L.F., and HosseinNia, S.H. (2022). Generalizing Hybrid Integrator-Gain Systems Using Fractional Calculus. In *IEEE Conference on Control Technology and Applications*, 1050–1055.

Khalil, H.K. (1996). Nonlinear Systems. Prentice Hall.
Matignon, D. (1996). Stability results for fractional differential equations with applications to control processing.
In Multiconference on Computational Engineering in Systems Applications, 963–968.

Monje, C., Chen, Y., Vinagre, B., Xue, D., and Feliu, V. (2010). Fractional-Order Systems and Controls: Fundamentals and Applications. Springer.

Podlubny, I. (1999). Fractional Differential Equations. Acad. Press.

Tepljakov, A., Petlenkov, E., and Belikov, J. (2011). Fomcon: Fractional-order modeling and control toolbox for matlab. In 18th International Conference on Mixed Design of Integrated Circuits and Systems, 684–689.

Trigeassou, J.C., Maamri, N., Sabatier, J., and Oustaloup, A. (2012). Transients of fractional-order integrator and derivatives. *Signal, Image and Video Processing*, 6(3), 359–372.

Trigeassou, J.C. (2019). Analysis, modeling and stability of fractional order differential systems 1. Wiley and Sons. Trigeassou, J.C. and Maamri, N. (2019). Analysis, model-

ing and stability of fractional order differential systems 2. Wiley and Sons.

Van Den Eijnden, S., Heertjes, M., Nijmeijer, H., and Heemels, W.M. (2024). Stability analysis of hybrid integrator-gain systems: A frequency-domain approach. *Automatica*, 164, 111641.

van der Schaft, A. (2017). L2-Gain and Passivity Techniques in Nonlinear Control. Springer Cham.

van Loon, S., Gruntjens, K., Heertjes, M., van de Wouw, N., and Heemels, W. (2017). Frequency-domain tools for stability analysis of reset control systems. *Automatica*, 82, 101–108.

Weise, C., Wulff, K., Hosseini, S.A., Kaczmarek, M.B., HosseinNia, S.H., and Reger, J. (2025). Fractional-Order Memory-Reset Hybrid Integrator-Gain System - Part I: Frequency Domain Properties. In *IFAC Symposium on Robust Control Design*.